Limnol. Oceanogr., 47(3), 2002, 906–910

Surface seiches in lakes of complex geometry

Abstract—In lakes of small to medium size, the characteristic frequencies of free oscillations of the water surface (seiches) depend only on the basin geometry. In irregularly shaped basins, such as dendritic reservoirs and multibasin lakes, these characteristic frequencies are not easily determined with simple formulas. Clear Lake, a multibasin lake in Northern California, is presented here as a case in point. The signature of the seiches in Clear Lake were only revealed after solving the eigenvalue problem governing the structure and frequency of seiches derived from the linear and frictionless depth-averaged shallow water equations in a nonrotating frame.

Many systems in nature have a built-in restoring force for re-establishing an equilibrium position following a perturbation. If the system possesses sufficient inertia, it will overshoot its equilibrium position and display free oscillations until friction damps out all motion. The free oscillations are characteristic of the system and are independent of the exciting force, except for the initial magnitude. A seiche is such an oscillation of the free surface in bodies of fluid enclosed wholly or partially by boundaries (Wilson 1972). The restoring force is provided by gravity, which returns the fluid surface to its horizontal equilibrium position after it is displaced by wind or pressure variations.

Seiches form by reflection of long progressive surface gravity waves by the boundaries. The free surface oscillates up and down with frequency ω, with the velocity being 90° out of phase. The amplitude of the oscillations varies in space but is fixed in time: lines of zero surface displacement are called nodes, whereas lines of maximum amplitude are called antinodes. Only certain discrete values of wavelengths and frequencies occur (*see* p. 208 in Kundu 1990), which, in the case of lakes of small to medium size where rotational effects are negligible, are strictly determined by the geometry of the containing basin. In the simplest case of a rectangular basin of length L and uniform depth H, the allowable wavelengths λ and periods T ($=2\pi/\omega$) of the seiches are

$$\lambda = \frac{2L}{N} \qquad N = 1, 2, \ldots \tag{1}$$

$$T = \frac{2L}{N\sqrt{gH}} \qquad N = 1, 2, \ldots \tag{2}$$

Here, g is the acceleration of gravity and N indicates the number of nodes. For the largest wavelength seiche ($\lambda = 2L$), Eq. 2, known as Merian's formula, describes the fundamental or first mode of oscillation. The oscillations would be binodal if $\lambda = L$, and trinodal if $\lambda = 2L/3$. Many of these higher modes of oscillation coexist with the fundamental mode in lakes.

Merian's formula can be used to estimate the periods of the dominant seiches in lakes of irregular depth and, if the geometry of the basin is relatively simple, using the mean depth and the length along the prevailing wind direction as characteristic scales. Unfortunately, its applicability to lakes and reservoirs with multiple basins or complex shape is very limited because a unique length scale is not easily defined. Furthermore, that simplified model does not provide a realistic description of the spatial structure of the seiches, which can have a strong influence on the erosion and transport of suspended sediments (Mei et al. 1997).

Clear Lake, in the Central Coastal Range of Northern California, is an example of a lake where Eq. 2 fails because of the complexity of the basin (Fig. 1). There are three distinct subbasins or arms: the Upper arm, the Lower arm, and the Oaks arm. At the east end of the Upper arm, a narrow passage (the Narrows) connects with the two other arms, which are considerably narrower and deeper. A summary of the lake's physical parameters is provided in Table 1. Wind is the main forcing mechanism of lake motions and has a very characteristic diurnal periodicity. On a typical winter day, the wind is from the northwest at 1–4 m s^{-1}, shifting to the east at 1–2 m s^{-1} in the afternoon. On a typical summer day, the winds are primarily from the northwest, mini-

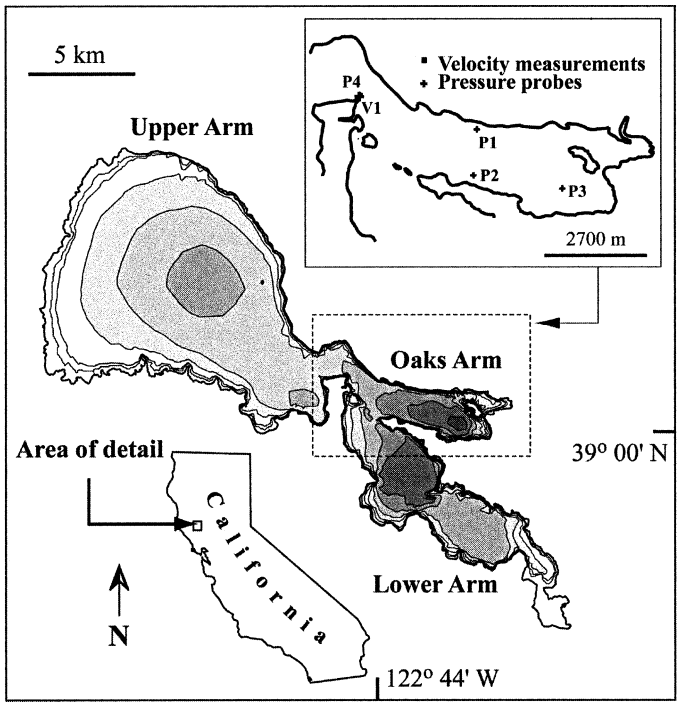

Fig. 1. Geographic setting and map of Clear Lake, Northern California. Contours shown in the bathymetric map are every 2 m. Also shown in the upper right corner are the location of measurement stations in the Oaks arm of Clear Lake during the field experiments of 1997 and 1999. Stations measuring pressure are identified with the letter P; those sampling water currents are identified with a V.

Table 1. Clear Lake physical parameters.

Basin	Area (ha)	Depth (m)		Shoreline (km)	Fetch		Width (km)	Volume ($\times 10^6$ m^3)
		Mean	Maximum		Length (km)	Axis		
Upper arm	12,700	7.1	12.2	56	16.4	SE–NW	12.2	904
Lower arm	3,270	10.3	18.4	39	13.4	SE–NW	4.3	384
Oaks arm	1,250	11.1	18.4	19	8.5	E–W	2.6	138
Overall	17,760	8.1	18.4	114	—	—	—	1,426

mal between midnight and dawn, and reach a maximum of 6 m s^{-1} at about dusk. A more complete description of the lake is available in Rueda (2001).

The problem of identifying the characteristic frequency of the modes of oscillations and their spatial structure was initially motivated by the need to interpret velocity observations gathered with an Acoustic Doppler Current Profiler in 1995 and 1997 in Clear Lake (Lynch 1996; Rueda 2001). Spectral analysis revealed a strong peak at about 3 h (0.3–0.4 cycles per hour (cph)) (Fig. 2). Under nonstratified conditions in November 1995, the magnitudes of the 3-h velocity oscillations were of the same order as the mean currents at the Narrows (approximately equal to 5 cm s^{-1}, Lynch 1996). The bottom boundary layer associated with such an oscillatory motion can potentially provide a significant mixing mechanism. The thickness (δ) of the oscillatory bottom boundary layer close to the Narrows estimated from the observed amplitude and the period of the oscillations (*see* p. 186 in Fischer et al. 1979) is approximately 0.5–1 m, which is a significant fraction (10%) of the water depth. A careful analysis of the 3-h band-pass–filtered signal in the velocity records of 1997 showed that it was in phase for all depths (Fig. 3), revealing its barotropic nature. The estimated damping time for these oscillations is approximately 24–48 h (*see* p. 186 in Fischer et al. 1979), and this suggests that seiches are effective mechanisms for extending the effects of the wind forcing in time.

None of the fundamental seiches for each of the arms, estimated with Merian's formula and their mean geometric characteristics, was near the 3-h periodicity observed in the data. Given that in most lakes and reservoirs water moves slower than gravity waves, the seiche signal (surface gravity waves) will be able to travel freely through the Narrows. Using Merian's formula to estimate the period of the first mode based on the combined length of the Upper and Lower Arms (18 km, which is the surface area of each divided by their mean width) and their overall mean depth (8.4 m), gives a period of 1.1 h, far from that observed. Clearly, a more sophisticated method is required. One such method, incorporating the effects of arbitrary shape and bathymetric variations and the Earth's rotation (Coriolis effects), was proposed by Rao and Schwab 1976 (*see* also Hamblin 1982) and applied successfully to Lakes Ontario and Superior. Although that method is the most general, the problem can be considerably simplified in basins of small to medium size, such as Clear Lake, where the effects of the Earth's rotation can be neglected (Wilson 1972). For Clear Lake, located at

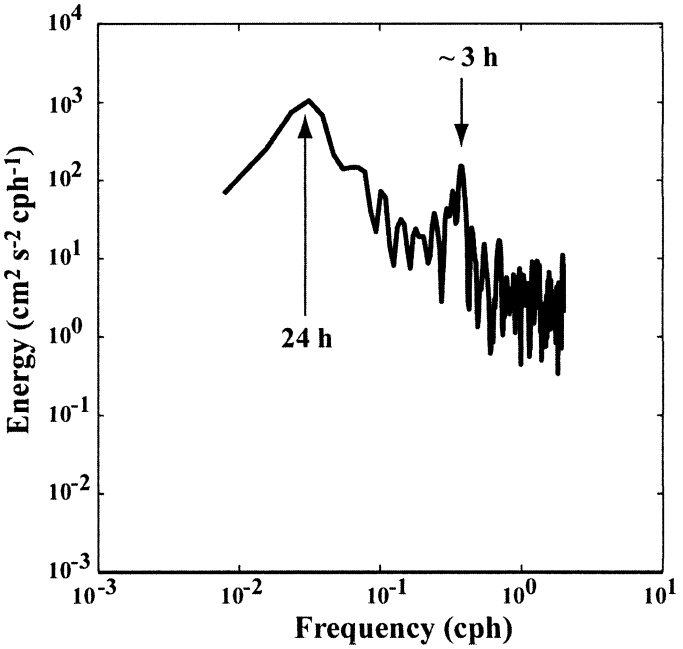

Fig. 2. Total energy in the power spectrum density of velocity at the Narrows. Velocity observations were gathered between 2 and 3 m below the surface at station V1 (Fig. 1) during 4 d in 1997.

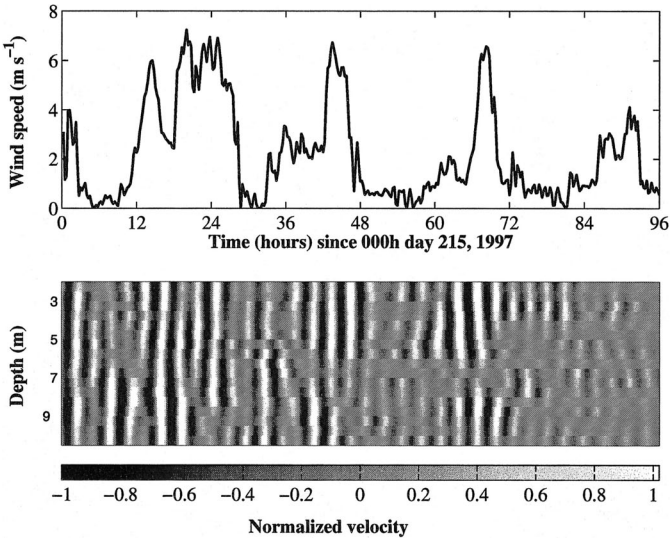

Fig. 3. Time series of wind speed (top) and band-pass–filtered velocity profiles at the Narrows in Clear Lake (bottom) during 4 d in August 1997. The magnitude of the filtered velocity component is normalized and is represented by the gray scale.

40°N and with a mean depth of 8 m, the Rossby radius of deformation (which defines a characteristic length scale for rotational effects) is approximately 100 km, much larger than its size. If one restricts the search to oscillations of small amplitude and neglects friction, it can be shown (Wilson 1972) that the spatial structure and periodicity of seiches in lakes of arbitrary geometry is governed by the following mathematical problem.

$$\frac{\partial}{\partial x}\left(H\frac{\partial \zeta}{\partial x}\right) + \frac{\partial}{\partial y}\left(H\frac{\partial \zeta}{\partial y}\right) + \left(\frac{\omega^2}{g}\right)\zeta = 0 \tag{3}$$

Here, H is the spatially varying basin depth, ζ represents the free surface displacement from an equilibrium position, and x and y are the coordinate directions in the horizontal plane. This equation is subject to the boundary condition

$$\partial\zeta/\partial n = 0 \tag{4}$$

where n denotes the normal direction and states that there can be no flow across the boundary surrounding the basin.

The differential eigenvalue problem in Eqs. 3 and 4 was discretized using the Galerkin weighted residual formulation of the finite element method (FEM; Fletcher 1991). This approach allows for (1) a more accurate representation of complex domains with fewer computational nodes than with finite difference methods and (2) a natural and straightforward implementation of the boundary conditions in Eq. 4. In the FEM the computational domain (Ω) is represented as a collection of simple domains called elements. Over each element, an approximate solution to the problem is constructed in the form

$$\hat{\zeta}(x, y, t) = \sum_{j=1}^{n} \zeta_j(t)N_j(x, y) \tag{5}$$

where $N_j(x, y)$ are basis functions and $\zeta_j(t)$ are the approximate values of variable ζ at n points called nodes. The basis functions are linear, and the elements are triangles, with the computational nodes located at the vertices. The elements are defined using isoparametric approximations; that is, the basis or interpolation functions are used to map an irregular element in the physical domain into a ''master'' element of fixed and regular shape (Reddy 1993). When substituted, the approximate solution Eq. 5 for ζ in Eq. 3 it will give a residual of the following form.

$$R(x, y) = \frac{\partial}{\partial x}\left(H\frac{\partial \hat{\zeta}}{\partial x}\right) + \frac{\partial}{\partial y}\left(H\frac{\partial \hat{\zeta}}{\partial y}\right) + \left(\frac{\omega^2}{g}\right)\hat{\zeta} \tag{6}$$

The residual in the Galerkin method is made orthogonal to all the interpolation functions $N_i(x, y)$.

$$\int_\Omega \left[\frac{\partial}{\partial x}\left(H\frac{\partial \hat{\zeta}}{\partial x}\right) + \frac{\partial}{\partial y}\left(H\frac{\partial \hat{\zeta}}{\partial y}\right) + \left(\frac{\omega^2}{g}\right)\hat{\zeta}\right]N_i(x, y)\, dx\, dy = 0$$
$$i = 1, \ldots, M \tag{7}$$

M represents the number of nodes in the computational domain. Integrating by parts, the above expression can be simplified to the following form.

$$\int_\Omega R(x, y)N_i(x, y)\, dx\, dy$$
$$= \int_\Omega \left[-H\left(\frac{\partial \hat{\zeta}}{\partial x}\frac{\partial N_i}{\partial x} + \frac{\partial \hat{\zeta}}{\partial y}\frac{\partial N_i}{\partial y}\right) + \frac{\omega^2}{g}\hat{\zeta}N_i\right] dx\, dy$$
$$+ \int_{\delta\Omega} H\left[\frac{\partial \hat{\zeta}}{\partial x}n_x + \frac{\partial \hat{\zeta}}{\partial y}n_y\right]N_i\, d\sigma = 0$$
$$i = 1, \ldots, M \tag{8}$$

Here, $\delta\Omega$ is the boundary of the domain where normal flux boundary conditions are specified, σ is a generalized variable representing distance along the boundary in a counterclockwise sense, and n_x and n_y are the components of a unit vector outwardly normal to $\delta\Omega$. For enclosed basins, the boundary condition that has to be satisfied along the whole boundary of the solution domain is zero normal flux; hence, the second integral term is identically zero.

As a result of discretizing Eqs. 3 and 4 with a finite element mesh of M nodes, an algebraic eigenvalue problem of the form

$$\mathbf{Av} = \mathbf{BvD} \tag{9}$$

is produced. Here **A** is referred to as the stiffness matrix and **B** is the mass matrix. Their elements obey the expressions

$$A_{ij} = -\int_\Omega H\left[\frac{\partial N_i}{\partial x}\frac{\partial N_j}{\partial x} + \frac{\partial N_i}{\partial y}\frac{\partial N_j}{\partial y}\right] dx\, dy$$
$$B_{ij} = -\int_{\delta\Omega} H[N_iN_j]\, dx\, dy \tag{10}$$

Such an algebraic problem is only satisfied for M values of ω^2/g (the eigenvalues) and M vectors **v** (eigenvectors). **D** in Eq. 9 is a diagonal matrix with the eigenvalues along its main diagonal. They determine the characteristic periods for the different modes of barotropic oscillations in the enclosed basin. The components of the eigenvectors represent the unknown amplitudes of the water surface elevation displacements at the nodes of the finite element grid (ζ_j). A MATLAB routine and an example application are presented in Web Appendix 1 (http://www.aslo.org/lo/toc/vol_47/issue_3/0906a1.pdf). Once the spatial structure of the water surface oscillations is determined by solving Eqs. 3 and 4, the linear frictionless depth-averaged shallow water equations (Lamb 1945) can be used to give the structure of the oscillation in the velocity field. In general, the nodes in the water surface oscillations correspond to the antinodes of the velocity.

A total of 418 computational nodes were employed to define the geometry of the Clear Lake basin. The frequencies of the first six modes are defined in Table 2. The spatial structure of the first and fifth modes is plotted along with the finite element mesh in Fig. 4. The inverse gray intensity

Table 2. Period of the first modes of barotropic oscillations in Clear Lake, given by the finite element code described in this appendix.

Mode	Period (h)
I	2.49
II	1.09
III	0.84
IV	0.78
V	0.61
VI	0.52

represents, in logarithmic scale, the normalized amplitude of the free surface oscillations (normalized against the maximum calculated amplitude). Primary interest is in the relative magnitude of the oscillations. The dark areas denote areas where the water surface is subject to low- or even zero-amplitude oscillations and depict the nodes of the seiches. The clear areas define areas of pronounced free surface oscillations or antinodes. It is clear from these figures that the results are far more complex than would be predicted from application of Merian's formula. Of particular note is the rapid variation in elevation in the vicinity of the Narrows, as seen for example in the mode I result. This is mainly the result of the abrupt change in lake geometry in that region, and it marks a region of significant velocity oscillations. It is in this area that the signature of the first mode seiche in the velocity signal is the strongest and even becomes the dominant feature in the hydrodynamic observations (Lynch 1996).

Four autonomously recording 9311 pressure loggers from Oregon Environmental Instruments were deployed in the Oaks Arm during 2 weeks in May 1999 to provide direct measurements of the oscillations of the free surface. The locations of the instruments are shown in Fig. 1, and they are denoted as P1–P4. The Alpha-Omega pressure sensors have an accuracy of 70 Pa and a resolution of 7 Pa in a range of water depths from 0 to 15 m, sampled at 1/60 Hz (i.e., 1 min between consecutive records). Unlike temperature or velocity sensors, which record changes due to a range of hydrodynamic processes, pressure sensors respond primarily to the changes in the surface elevation caused by surface seiches. Figure 5 shows the power spectrum density of the water surface elevation records collected at the four stations (P1–P4). The vertical bars at the top of the figures are the frequencies of the seiches calculated with the model and agree with the peaks in the spectra. In all of the pressure records there exist two peaks at periods of 24 and about 2.5–3 h. The 24-h peak is due to the diurnal wind events, mostly from the northwest, which push water downwind, causing the surface to rise at the eastern end of the Oaks arm. This peak is therefore especially strong at the downwind end of the lake (station P3). The 3-h peak corresponds to the first barotropic mode or fundamental seiche. Figure 4a shows that a node for water surface oscillations is located in the vicinity of the Narrows, and accordingly, the power of the 3-h peak at station P4 (Fig. 5) is the lowest of the four stations. Other peaks can be similarly identified in the spectrum, which

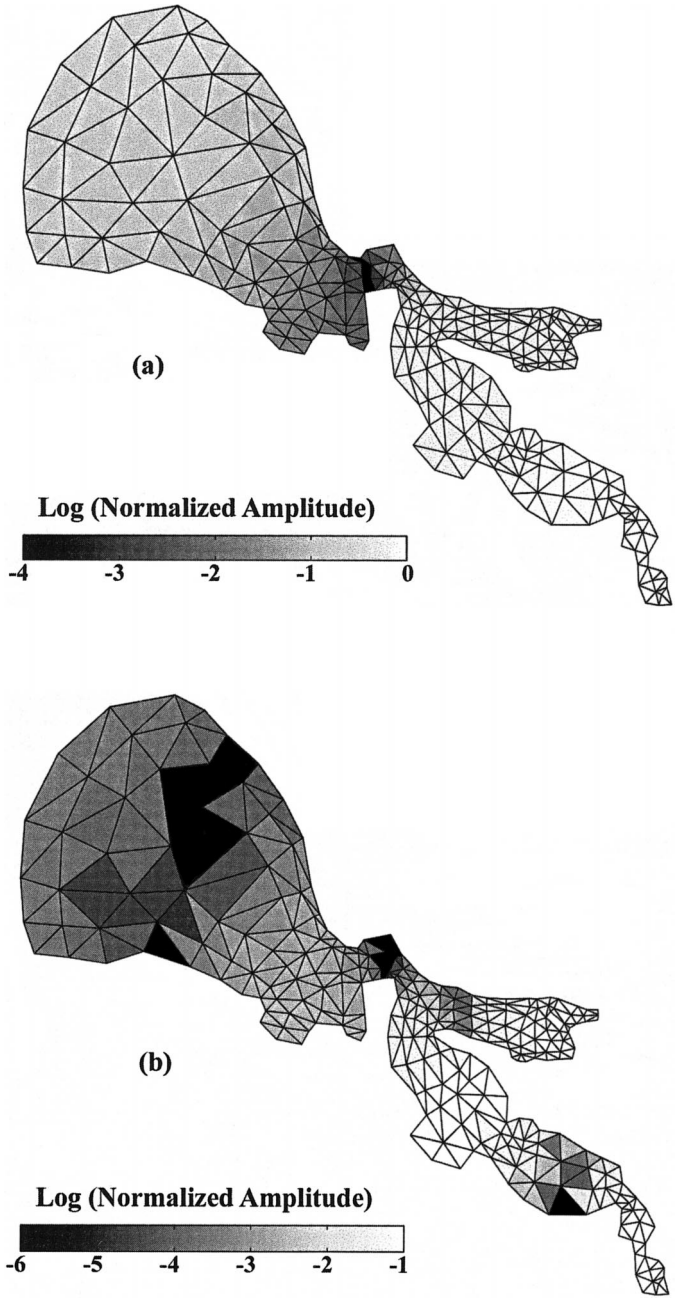

Fig. 4. Spatial distribution of the amplitude of the first modes of oscillations of the free surface, as calculated by the finite element model. (a) Fundamental seiche; (b) sixth barotropic mode.

correspond to higher modes of oscillations. The surface mode of oscillation at the 0.52-h period (Fig. 4b) provides an excellent example of the spatial variation of the magnitude of the oscillations captured by an array of pressure sensors. A node of this mode is located across the Oaks Arm at its center, close to stations P1 and P2, and accordingly, the peak at 2 cph does not appear in the spectra of the water surface elevations at stations P1 and P2, although it is quite conspicuous in the spectra from stations P3 and P4.

This work illustrates the difficulties encountered when try-

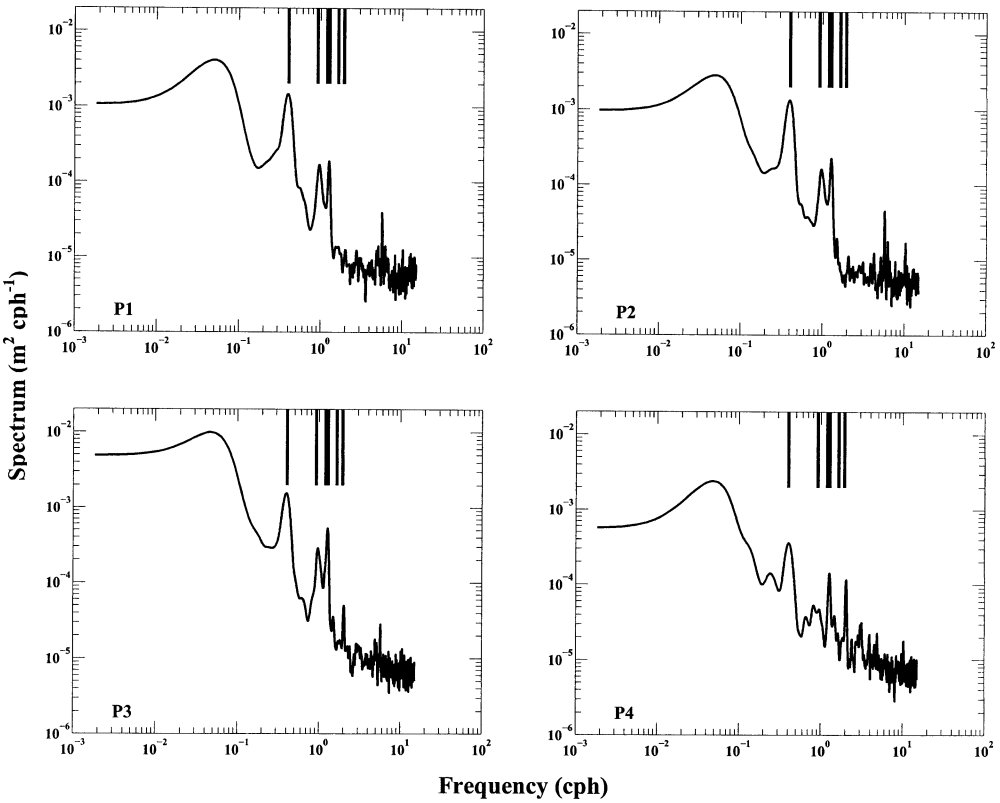

Fig. 5. Power spectrum of the free surface elevation signal at stations P1, P2, P3, and P4. The location of these stations is shown in Fig. 1.

ing to identify the signature of free oscillations of the water surface in lakes and reservoirs of complex geometry. Occasionally the purpose of making such an analysis is to remove unwanted frequencies to identify an underlying signal of interest from a time series. The results can also be used to select instrument locations in order to minimize or maximize the contribution of the seiche signal.

Francisco J. Rueda[1]
S. Geoffrey Schladow[2]

Department of Civil and Environmental Engineering
University of California
Davis, California 95616

[1] Present address: School of Civil and Environmental Engineering, 109 Hollister Hall, Cornell University, Ithaca, New York 14853.

[2] To whom correspondence should be addressed.

Acknowledgments

We thank the staff of the Clear Lake Environmental Research Center and students of the Environmental Dynamics Laboratory at U.C. Davis for their cooperation with the field component. This work was partially supported by the Spanish Ministry of Education and Culture, by the U.S. Environmental Protection Agency–sponsored Center for Ecological Health Research (CEHR) at U.C. Davis, by a grant from the U.S. EPA's Science to Achieve Results (STAR) program through grant GR825428-01-0, and by the U.C. Toxic Substances Research and Teaching Program.

References

FISCHER, H. B., E. J. LIST, R. C. Y. KOH, J. IMBERGER, AND N. H. BROOKS. 1979. Mixing in inland and coastal waters. Academic Press.

FLETCHER, C. A. J. 1991. Computational techniques for fluid dynamics. Springer.

HAMBLIN, P. F. 1982. On the free surface oscillations of Lake Ontario. Limnol. Oceanogr. **27:** 1039–1049.

KUNDU, P. K. 1990. Fluid mechanics. Prentice Hall.

LAMB, H. 1945. Hydrodynamics. Dover.

LYNCH, M. G. 1996. Seasonal variations in lake mixing, Clear Lake, California. M.S. thesis, Univ. of California, Davis.

MEI, C. C., S. FAN, AND D. JIN. 1997. Resuspension and transport of fine sediments by waves. J. Geophys. Res. **102:** 15,807–15,821.

RAO, D. B., AND D. J. SCHWAB. 1976. Two dimensional normal modes in arbitrary enclosed basins on a rotating earth: Application to lakes Ontario and Superior. Philos. Trans. R. Soc. Lond., A **281:** 63–96.

REDDY, J. N. 1993. An introduction to the finite element method. McGraw-Hill.

RUEDA, F. J. 2001. A three-dimensional hydrodynamic and transport model for lake environments. Ph.D. dissertation, Univ. of California, Davis.

WILSON, B. W. 1972. Seiches, p. 1–94. *In* Ven Te Chow [ed.], Advances in hydrosciences, 8. Academic Press.

Received: 24 July 2001
Accepted: 24 November 2001
Amended: 2 January 2002